# EFFECTS OF RADIO WAVE PROPAGATION IN URBANIZED AREAS ON UAV-GCS COMMAND AND CONTROL

Lock Wai Lek
Singapore Armed Forces
wlock@starnet.gov.sg

David C. Jenn
Naval Postgraduate School
Department of Electrical & Computer Engineering
833 Dyer Road
Room 437
Monterey, CA 93943
jenn@nps.navy.mil
831 656 2254

## ABSTRACT

In an urban environment, the linkage between UAVs and ground control stations are subjected to multipath interference due to reflection, diffraction, and scattering between the transmitter and receiver. Severe multipath can result in a nearly complete loss of command signals, which can limit the UAV's operational area or even cause a loss of the vehicle. This paper examines the propagation of RF signals through an urbanized area using a ray-tracing computational electromagnetics software package. Several scenarios were developed to approximate actual operational situations. Given the UAV's transmitter power and other system parameters, the signal levels are computed on a grid of specified observation points. Variations in the simulation included observation point locations, building material composition, building density, UAV operating altitude and frequency, number of deployed UAVs and their locations, and theoretical ray bounce considerations.

Based on a large number of simulations several guidelines for operating a UAV in a dense urban environment are suggested, such as how to select an optimum altitude and the potential use of "urban canyons" for communications.

## I. INTRODUCTION

Many armed forces around the world have recognized the tremendous potential of unmanned aerial vehicles (UAVs) for battlefield surveillance and reconnaissance. UAVs are remotely piloted or self-piloted aircraft that can carry cameras, sensors, communications equipment or other payloads. They have been used in reconnaissance and intelligence gathering roles since the 1950s and more challenging roles like combat missions are envisioned [1]. A study conducted by United States Office of the Secretary of Defence/C3I regarding the use of a UAV as an Airborne Communication Node (ACN) [2] concluded that tactical communication needs can be met much more responsively and effectively with ACNs than with satellites.

Because of the growing trend towards urbanization, future wars may no longer be fought on large expanses of open terrain like pastures and deserts, but in built-up areas. At the same time, the trend towards network centric warfare puts a high demand on battlefield comprehensive awareness for commanders and troops linked by communication and sensor nodes. Existing command and data links for UAVs are point-to-point communication links between the UAV and a ground control station (GCS). However, future concept of operations (CONOPS) would involve UAV or payload control from soldiers in units other than the controlling units. These operations require future systems to evolve from control center to network centric application.

UAV-GCS linkage in an urbanized area is subjected to multipath interference due to reflection, diffraction and scattering. Opaque or absorbing materials, corners of buildings, and window openings can cause large fluctuations in the signal. Shadow regions are formed when the line of sight (LOS) is blocked from radio-frequency (RF) signals. Severe multipath can result in a nearly complete loss of command signals, which can limit the operational area or even cause a loss of the vehicle. On the other hand, diffraction at edges and corners causes illumination behind obstructions, and spreading through small apertures, which can actually help in extending propagation in some cases.

This paper examines the propagation of RF signals through an urbanized area using a commercially available ray-tracing software package. Several scenarios were developed to approximate actual operational situations. Given the UAV's transmitter power and other system parameters, the signal levels are computed on a grid of specified observation points. Variations in the simulation included observation point locations, building material composition, building density, UAV operating altitude and frequency, number of deployed UAVs and their locations, and theoretical ray bounce considerations.

The signal strength level necessary to establish a link depends on the receiver sensitivity as well as interference and noise at the GCS. In order to make the contours system independent, the signal power levels are computed in decibels relative to a milliwatt (dBm). Once the specific parameters of the GCS are known, the contours that will satisfy the minimum signal strength requirements can be easily converted into operational range contours. Two common frequency bands used by existing UAVs were examined. They are 5 GHz (C band) and 15 GHz (Ku band) for line-of-sight (LOS) command, control, and data links.

## II. PROPAGATION MODELING

The mechanisms that govern radio propagation in urban areas are complicated, but they are generally attributed to three basic propagation methods: (1) reflection, (2) diffraction, and (3) scattering [3]. UAV-GCS command links in urban environments are subjected to severe degradation due to the superposition of these components. As a result, the received signal strength at the GCS can be roughly characterized by three nearly independent phenomena of large-scale path loss, large-scale shadowing, and multipath fading.

For most data and communication links, a narrow band sinusoidal case can be assumed where the time dependence is of the form $e^{jwt}$ ($w = 2p\, f$, $f$ is frequency, and $j = \sqrt{-1}$) so that phasor quantities can be used. Furthermore, because the reflecting and diffracting objects are large compared to the wavelength, high-frequency ray-tracing approximations can be applied, as shown in Figure 1. The received power $P_r$ at the GCS due to a UAV transmitting a power $P_t$ with antenna gain $G_t$ at range $R$ is given by the Friis equation [4]

$$P_r = \frac{P_t G_t G_r l^2 L G_p}{(4p)^2 R^2} |F|^2 . \qquad (1)$$

The wavelength is $l = c / f$, where $c = 3 \times 10^8$ m/s is the phase velocity in free space. The GCS antenna gain in the direction of the UAV is $G_r$. The miscellaneous loss and processing gain factors, $L$ and $G_p$, respectively, are system dependent.

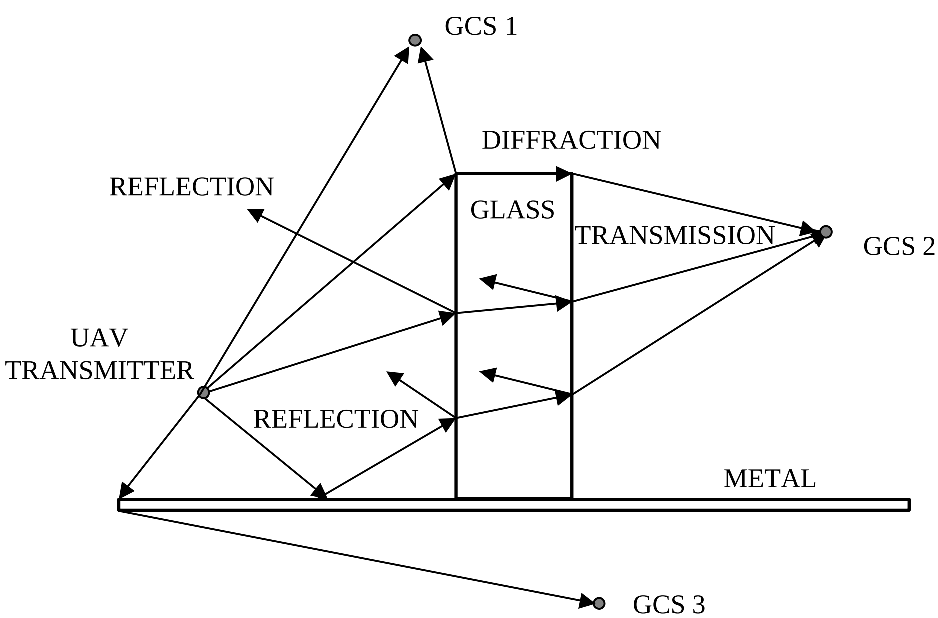


Figure 1: Illustration of some possible ray paths for the simple case of a glass slab and metal wall, for the case of the GCS transmitting.

The path-gain factor (PGF) $F$ gives the total electric field intensity at the GCS relative to the direct free-space electric field intensity. In addition to the direct path signal, for ray-based propagation modeling, the contributors to the total electric field intensity are the reflected and diffracted signals that occur in the environment. They arise from the ground and foliage, or buildings and other manmade objects on the ground or in the air. Given an observation point in space, the total field will be the sum of all of the direct, reflected, and diffracted fields arriving at that point.

Formulas are available for the reflected and diffracted fields based on geometrical optics (GO) and the geometrical theory of diffraction (GTD) [5]. They incorporate reflection (diffraction) coefficients that linearly relate the reflected (diffracted) fields to the incident fields at the reflection (diffraction) points. In the case of reflection, the traditional Fresnel coefficients for planar boundaries can be used [5]. Specular (mirror-like) reflections must satisfy Snell's law. The diffracted fields lie on a cone whose axis is coincident with the diffracting edge and half angle is determined by the angle of the incident ray with the edge. The number of terms needed for a converged value of $F$ in equation (1) must be determined from the minimum signal level that is to be reliably computed, and in an urban environment this is difficult to predict in advance.

The formulas for the reflection and diffraction coefficients depend on the electrical properties of the materials. The materials are defined by their complex relative permittivity ($e_r = e'_r - je''_r$), relative permeability ($m_r = m'_r - jm''_r$), and surface resistivity ($R_s$) [6]. Materials with infinitely large $R_s$ are transparent to waves while those with small $R_s$ ($\lesssim 50$) are highly reflective. Combinations of these parameters can be used to achieve the electrical characteristics of most common building materials.

While there are several engineering tools to predict antenna radiation and wave propagation, *Urbana* [7] was selected for this research. The propagation model is essentially a three-dimensional ray-tracing process that in principle predicts the local mean power received at any given point. For each observation point, reflection and diffraction points are determined, the ray paths between the transmitter and receiver are traced, and then the vector sum of multipath signals computed.

## III. SCENARIOS AND SIMULATION RESULTS

### A. UAV System Parameters

For the purpose of defining the simulation scenarios, the UAV is assumed to be similar to the multipurpose security and surveillance mission platform (MSSMP) [8]. It is capable of hovering, and designed to provide a rapidly deployable, extended-range surveillance capability for a variety of operations and missions.

A vertically polarized dipole antenna transmitting at 5 GHz with a power of 1 W was used to simulate a data signal from the MSSMP. The signal contours for other power levels can be determined by simple scaling, since all of the scattering phenomena and the media are linear. The receiving antenna pattern is isotropic, and the signal levels are plotted in dBm. A combination of GO and GTD were used in computing the signal contours. Single diffraction and up to seven reflections were included in the ray tracing. Mixed modes (e.g., reflected-diffracted rays) were not included.

### B. Central City Area

A number of urban environments were examined during the course of the research [9], however, only two general cases will be discussed here. The first, shown in Figure 2, is based on a sample file that is included with the *Urbana* software. It represents a central city area with a mix of high and low buildings. The tallest building (357 m) is in the category of a skyscraper, such as the Sears building in Chicago. The size of the observation plane ($x$-$y$ plane) is 1620 m by 800 m. The observation cell size is a square with edge lengths of 1 m. Therefore the “pixel” size for the resulting contour images is 1 m by 1 m. Since this is much greater than the wavelength of the frequencies under consideration, the field strength at other points in the cell will fluctuate about the center value. Small-scale variations in the field are not captured, but large-scale path loss and shadowing are. More resolution can be achieved at the expense of increased computation time.

For buildings comprised of several materials, an average value can be estimated based on the constituent materials. When both the transmission and reception points are outdoors, the details of the building walls (i.e., the locations of doors and window openings) are not as crucial to the computation as they are for outdoor-to-indoor and indoor-to-outdoor propagation. Therefore homogeneous exterior walls with averaged material properties are sufficient in most cases. Roads were simulated with a thin layer of concrete over a semi-infinite plane.

To illustrate the effect of different building materials, Figures 3 through 5 show the outdoor signal levels for buildings comprised predominately of concrete, glass and wood, respectively. The UAV is modeled at the open area near the right portion of the city coordinates $(x, y, z) = (-353 \text{ m}, -69 \text{ m}, 187 \text{ m})$.

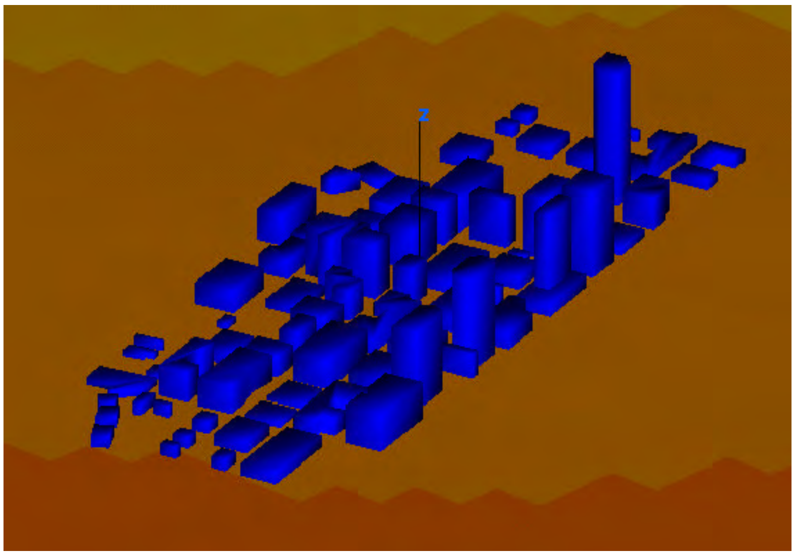


Figure 2. Model of a dense urban environment. (From reference [7].)

Figure 3. City with predominately concrete buildings (distance unit is meters).

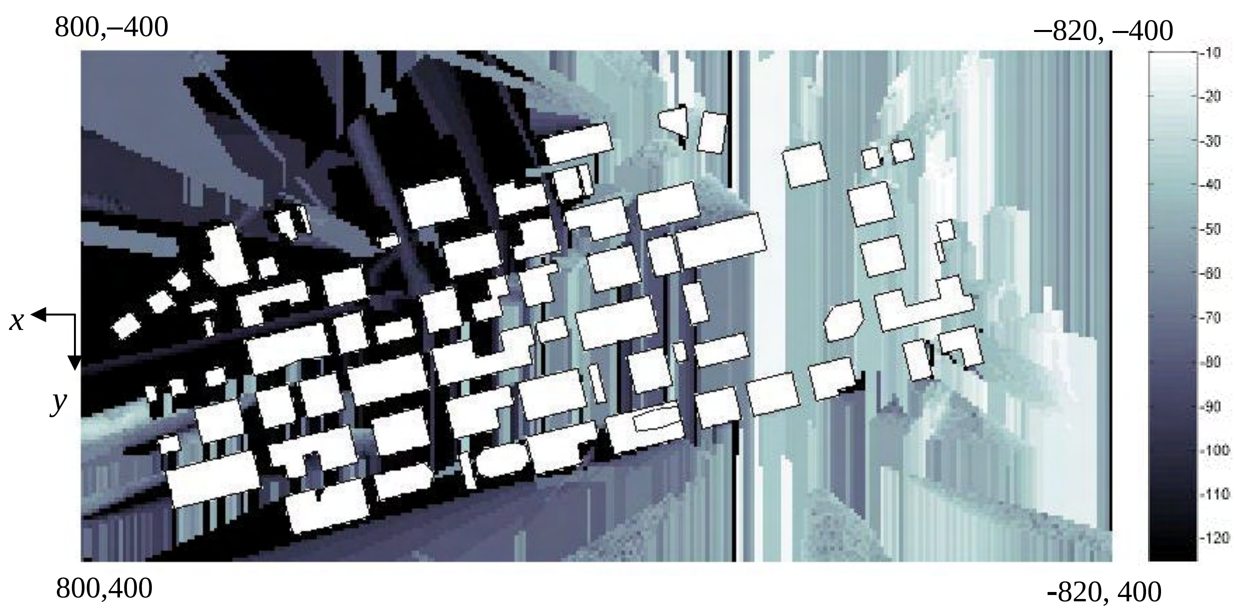

Figure 4. City with predominately glass buildings (distance unit is meters).

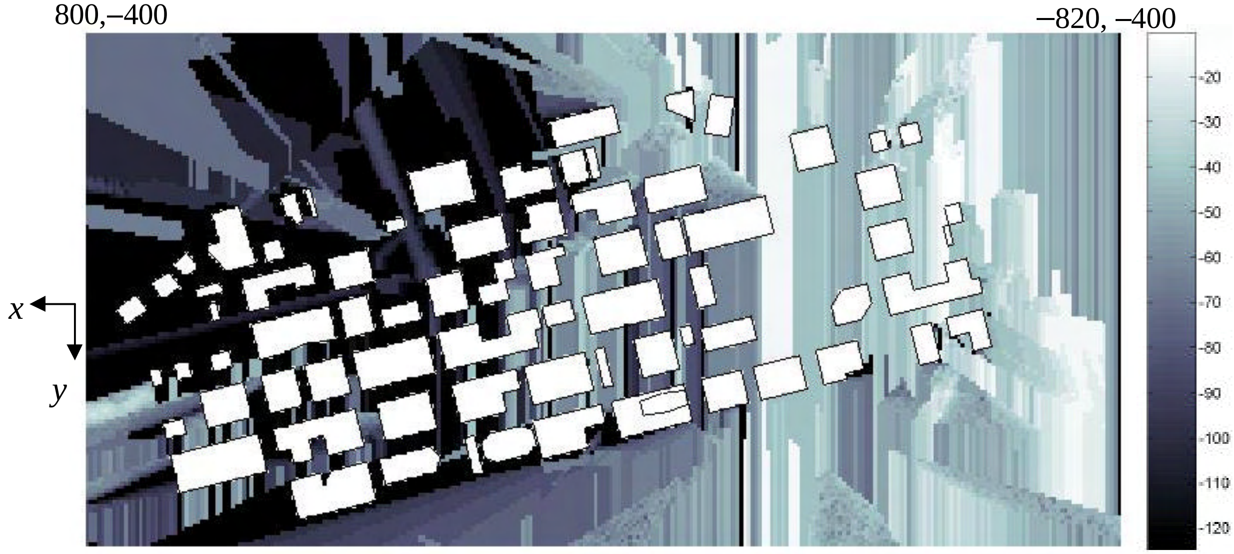


Figure 5. City with predominately wood buildings (distance unit is meters).

The results demonstrate that building materials have a significant effect on the signal contours. In the concrete model shown in Figure 3, propagation is limited to the open areas with large regions being shadowed. However, in Figures 4 and 5, due to a higher transparency of the building materials, there is more transmission through the buildings.

**C. Ducted Waves in an Urban Canyon**

A main feature of an urbanized area is the presence of long straight avenues of roads and pavements with high buildings on both sides, thus forming a so-called “urban canyon.” Analogous to surface wave ducting in the atmosphere [10], waves are trapped in the canyon and propagate extended distances with little attenuation. The effect of urban canyons is clearly visible in Figure 6 as a corridor for strong radio-wave propagation. For this calculation metal buildings were used and the UAV was located at (752 m, 203 m, 150 m). The buildings are acting as a waveguide, effectively preventing the signal from dispersing.

These data indicate that in certain parts of the city, despite having no LOS, troops are still able to receive and transmit with higher headquarters (HHQ) through ACNs. Tactically, identification of urban canyons becomes important for total communications coverage throughout the military operation with the minimal logistics tail.

**D. Flying a UAV Over a City**

In this scenario, the UAV is flown over the city along the *x*-axis in support of troops advancing from the right. The altitude of the UAV is kept constant at 358 m, which is just above the tallest building in the city. The *y*-coordinate is maintained constant at $-7$ m. Figures 7 to 9 represent a series of time snapshots that shows the signal contours in the city as the UAV moves along its flight path.

The figures clearly show the shifting of shadow regions. In order to achieve the required signal strength level for an effective UAV-GCS link, it is necessary to anticipate the changes of signal contours and to locate, if possible, the ideal position for the GCS. The figures suggest that, for low transmission powers, the location of the GCS will need to displace with the advance of the UAV. This scenario highlights the needs of a UAV deployed in support of MOUT should have the inherent capability to hover in order to capitalize on communications opportunities.

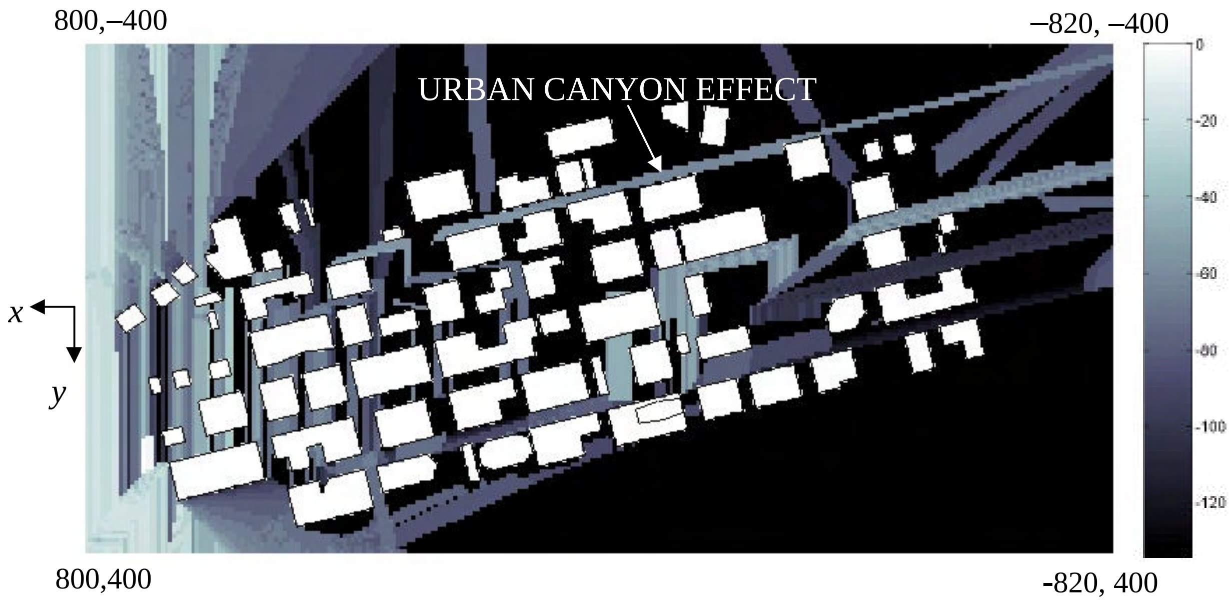


Figure 6. Example of strong propagation along streets of a city with predominately metal buildings (distance unit is meters).

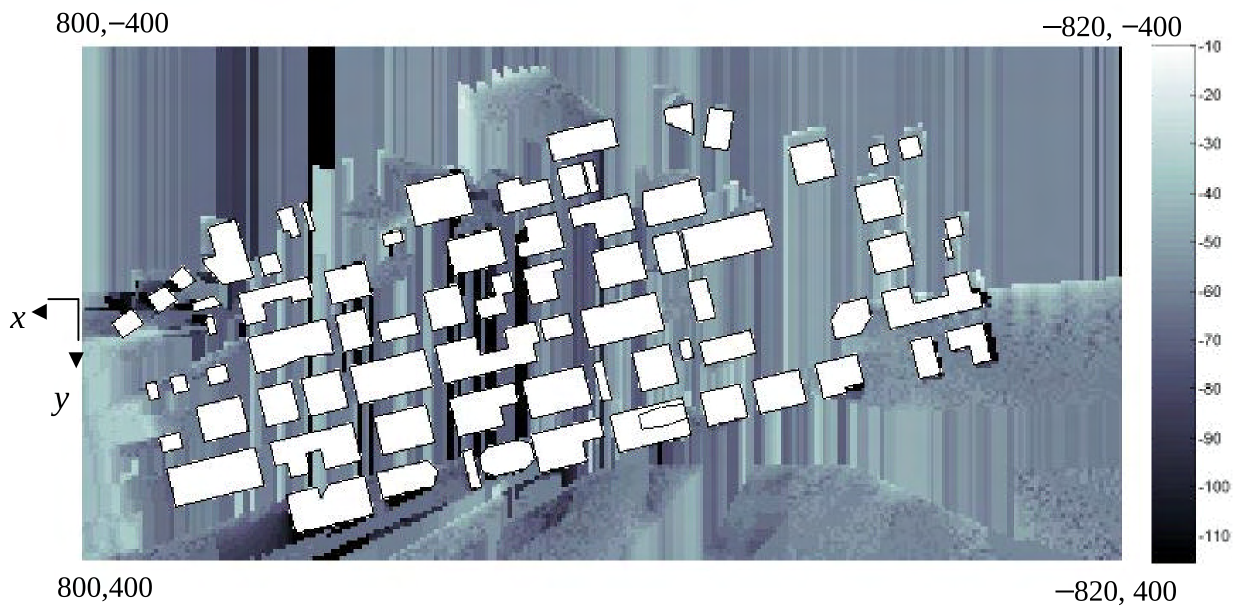


Figure 7. UAV flying over a city (currently at $x = -385$ m).

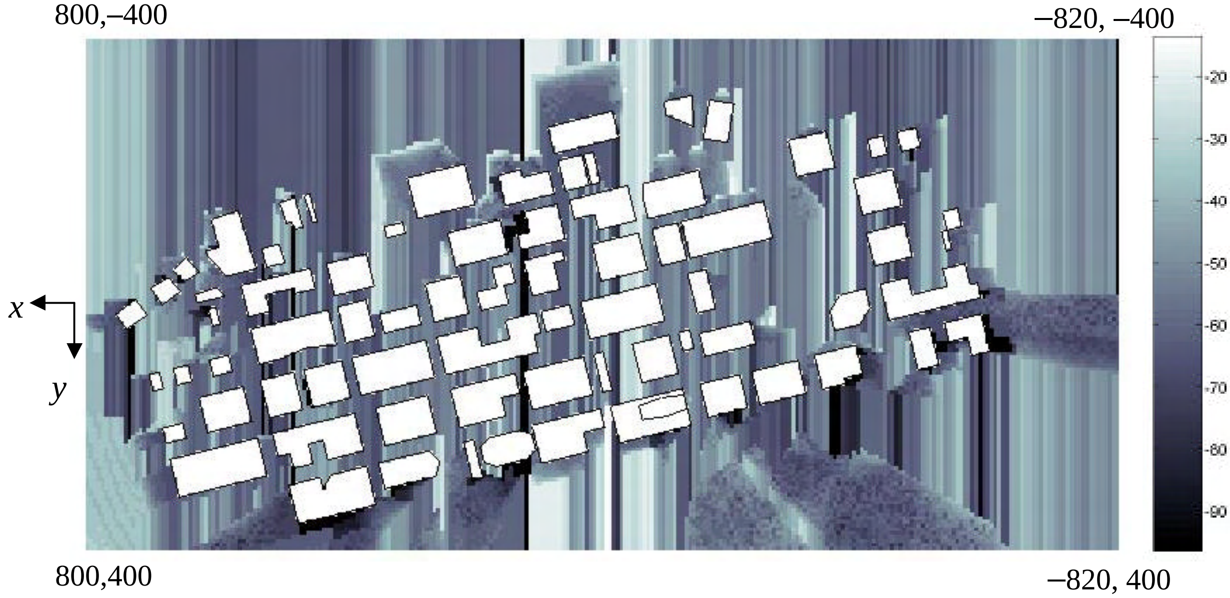

Figure 8. UAV flying over a city (currently at $x$ = 0 m).

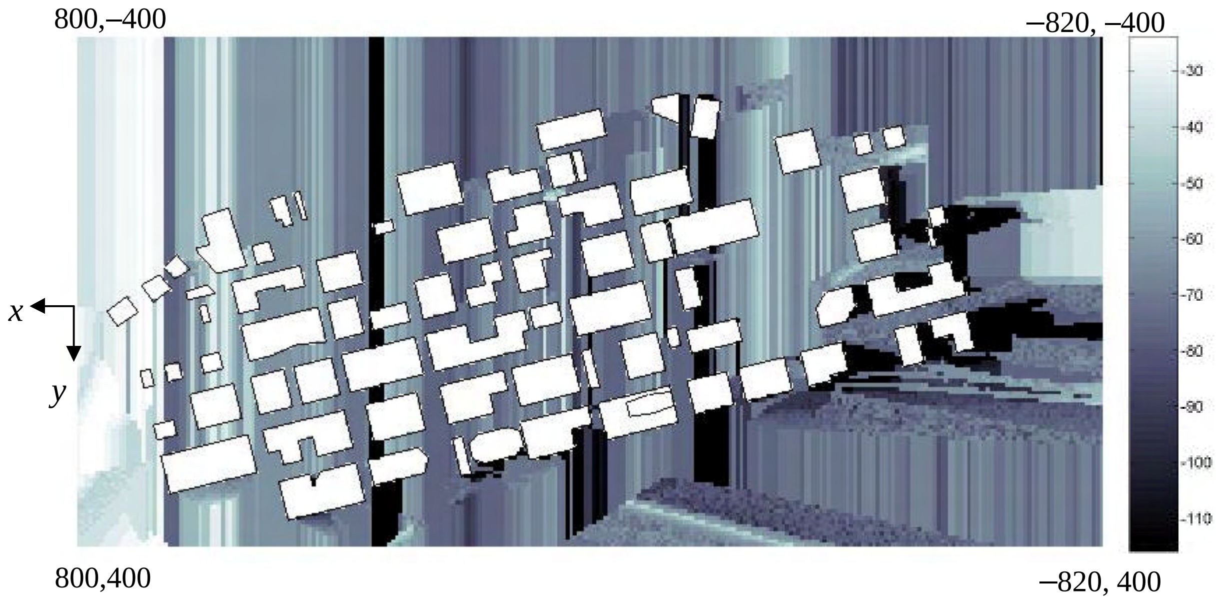

Figure 9. UAV flying over a city (currently at $x$ = 1200 m).

**E. Operating Altitude**

The UAV signal was examined for various flight altitudes. The location of the UAV is near the tallest building in the city $(x, y) = (-385$ m, $-10$ m). The $z$-coordinate was set at 1,000 m and 10,000 m with the resulting signal contours shown in Figures 10 and 11, respectively. At three times the height of the tallest building, coverage within the city using a single UAV provided better coverage contours than using two UAVs operating at lower altitudes or perched at rooftops. A larger grazing angle creates smaller shadow areas around buildings. However, a hovering UAV at high altitude will be consuming energy during flight as compared to one that is perched at rooftops on standby mode and will require considerable planning.

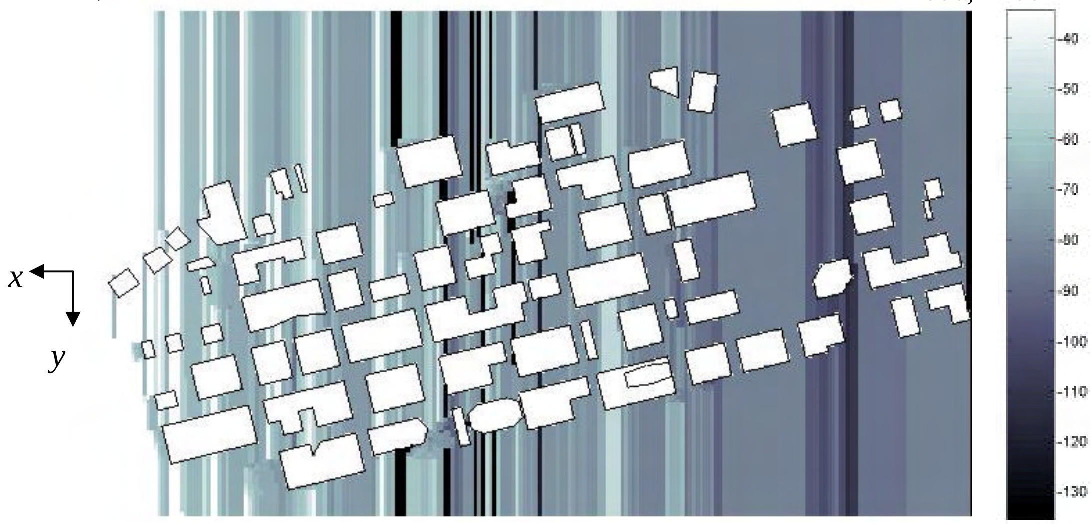


Figure 10. Varying UAV altitude ($z$ = 1,000 m).

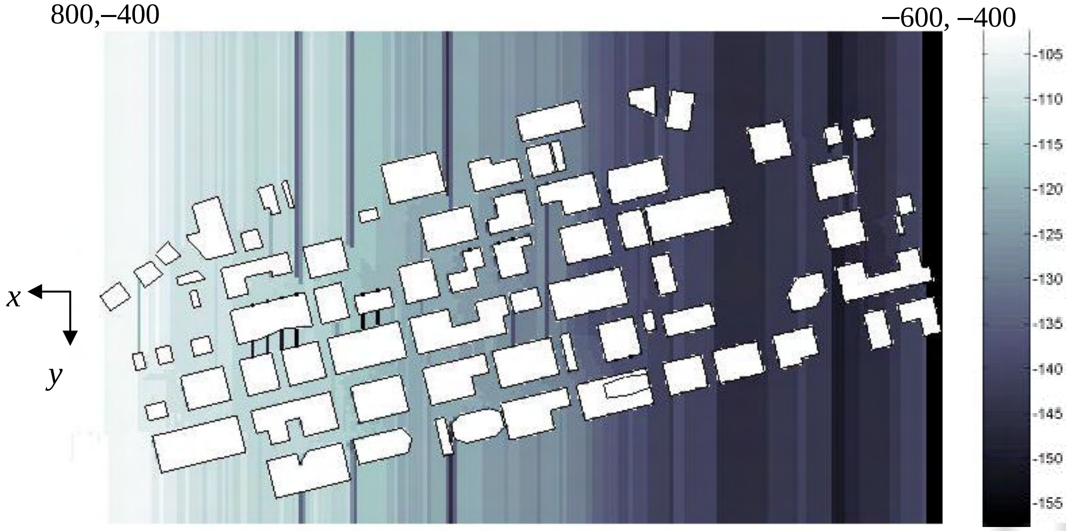


Figure 11. Varying UAV altitude ($z$ = 10,000 m).

Figure 11 shows that, at a high altitude, the area directly under the UAV antenna (in its null) will experience low signal levels, while locations further away are in a region of higher antenna gain. Path loss increases substantially at high altitudes, which must be compensated for by transmitting at a higher power. The advantage of operating at high altitude would be a larger area of uniform illumination, because shadows are smaller. Requirements for adaptive positioning of the GCS would subsequently diminish.

Note that no strong urban canyon effect was created at these altitudes. In order to effectively use an urban canyon for propagation, the transmitter must couple into the guiding structure. The coupling is most efficient when the height of the UAV is below the buildings forming the walls of the canyon. Thus positioning of the UAV is pivotal in utilizing the urban canyon effect.

### F. Frequency Dependence

Finally, the operating frequency of the UAV was varied to observe its effects on coverage. The location of the UAV was fixed at the tallest building (−385 m, −7 m, 358 m) and the frequency was set at 5 GHz and 15 GHz. The signal contours are shown in Figures 12 and 13, respectively.

Comparing both figures, it is observed that there is an insignificant change in signal contours, as long as the wavelength is small compared to the size of the buildings. This is not surprising because the low signal areas coincide with shadows. The nature of shadows is geometric, and therefore independent of frequency. However, the small-scale fluctuations will change with frequency, but they cannot be observed with the large cell size of 1 m. Calculations with a smaller cell size confirmed that the signal fluctuations across the width of a 1-m cell were typically in the range of 1 to 3 dB.

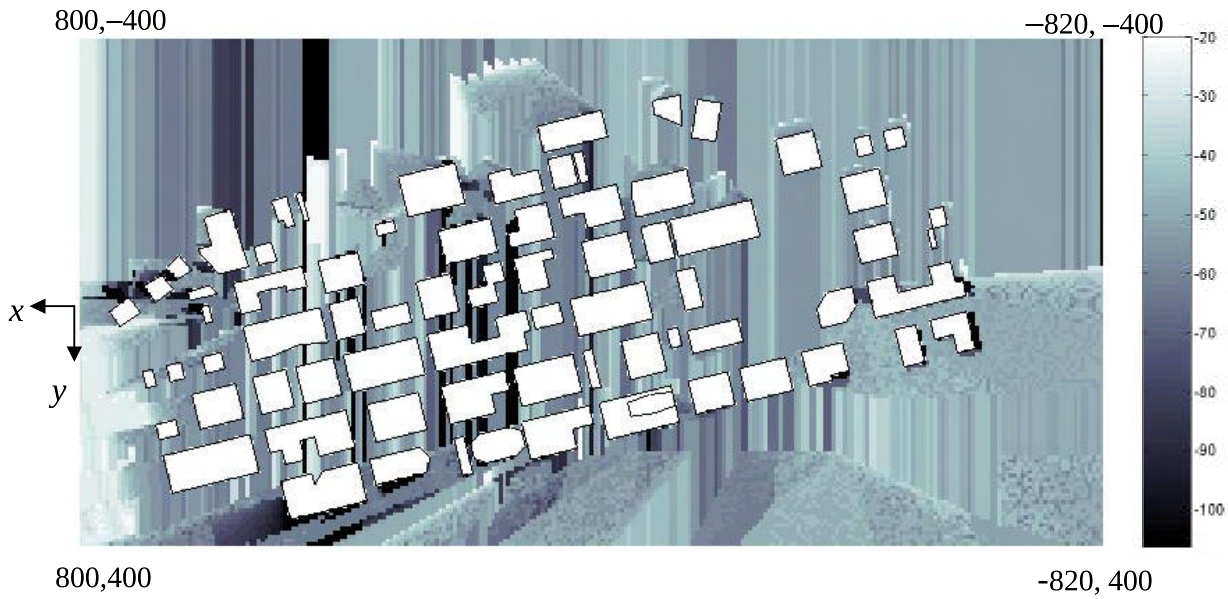


Figure 12. Signal distribution for a frequency of $f$ = 5 GHz.

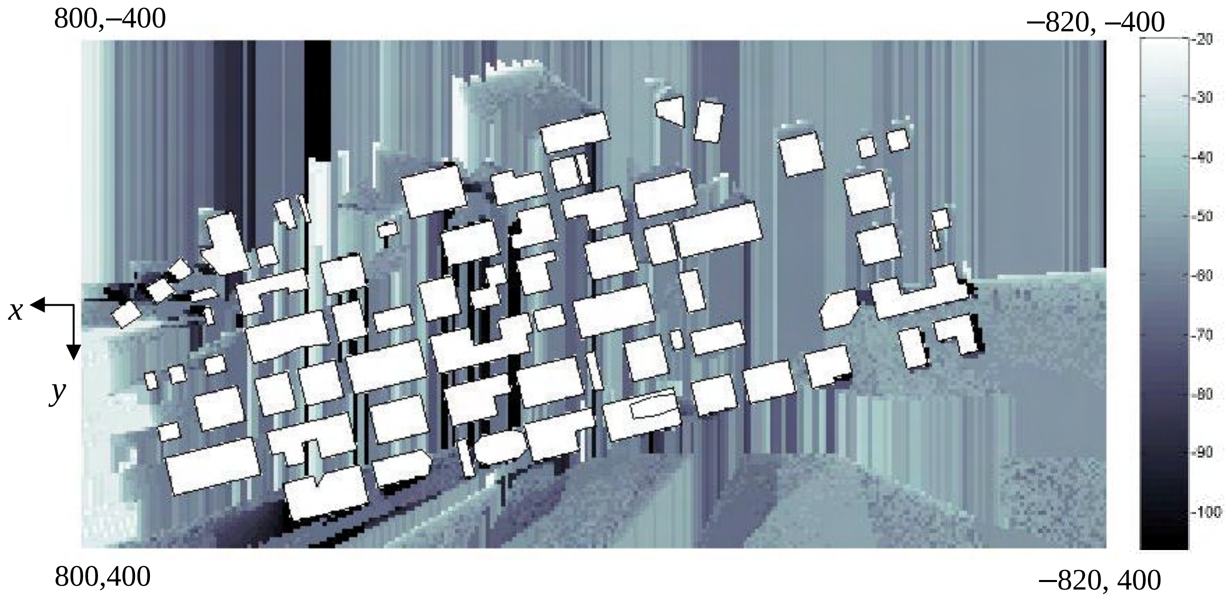


Figure 13. Signal distribution for a frequency of *f* = 15 GHz.

**G. Indoor Reception For GCS**

The second set of scenarios consisted of a series of single story buildings that might be used to house a portable GCS. The research focused on indoor reception of RF signals, as would be the case when a soldier operates from the safety of a building. One configuration is shown in Figure 14. The footprint of the base building is 800 inches by 800 inches with a wall height of 132 inches. The observation cell size is 12 inches by 12 inches and the observation plane for all of the simulations was set at mid-window level. Since outdoor-to-indoor propagation is being modeled, the window openings are included, and various window materials were considered. The barrier wall is of the same thickness as the walls of the buildings.

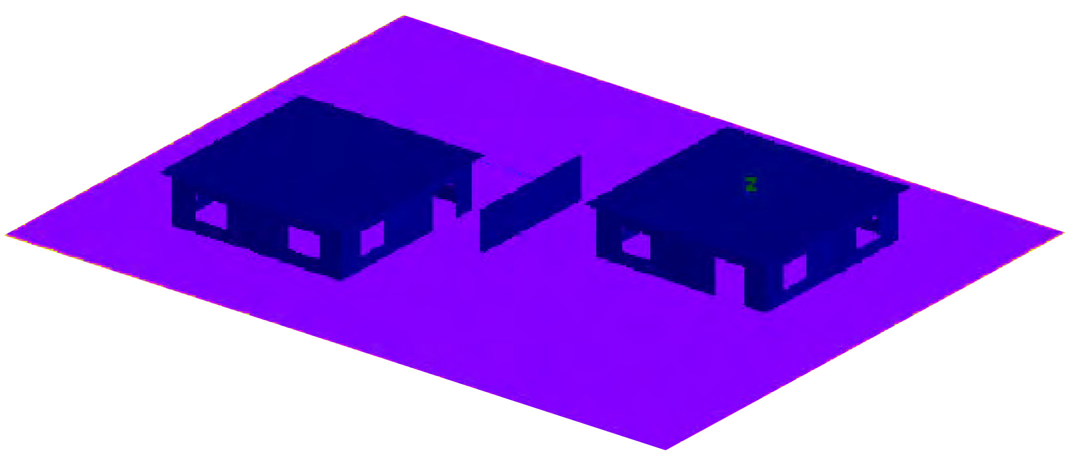

Figure 14. Two buildings with a barrier wall.

The signal contours are shown in Figure 15 for a UAV located at (504 inches, 354 inches, 250 inches). The strong transmission through the windows is evident, and it is these areas that offer the highest potential for good reception. Diffraction from the edges of windows, which propagates into the shadow regions, may also permit reception if the receiver sensitivity is sufficient. When the UAV is moved to (−50 inches, 450 inches, 400 inches) the signal contours shown in Figure 16 result. Instead of a pattern with stronger regions at windows, multipath inside of the building created a cross-like pattern with a significant signal level at the intersection. In this configuration, troops are able to operate a UAV away from windows, out of enemy fire.

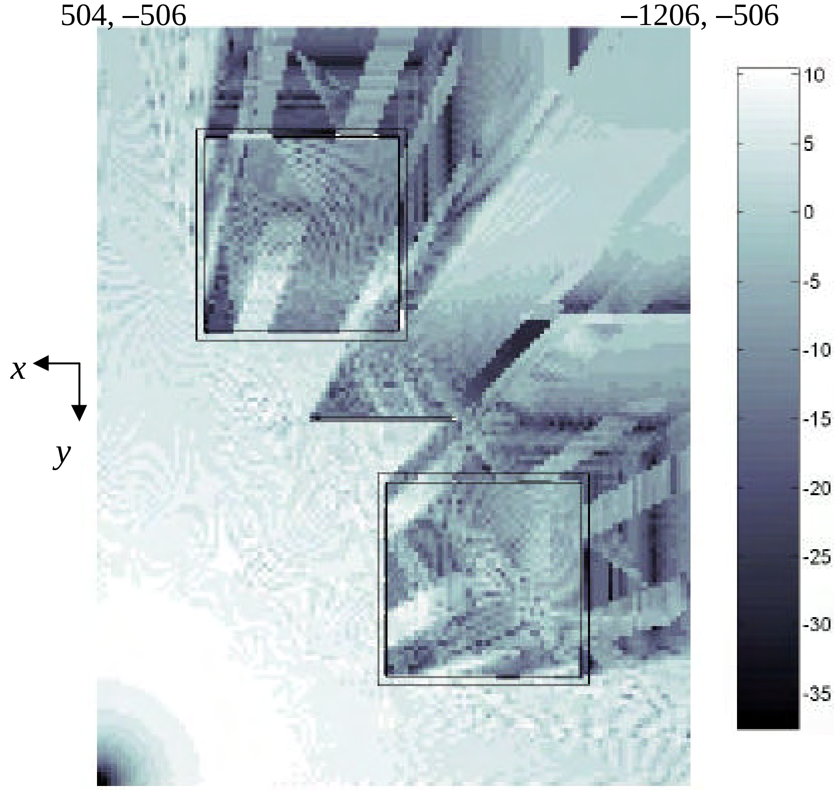


Figure 15. Two single level buildings with barrier wall with the UAV at (504 inches, 354 inches, 250 inches).

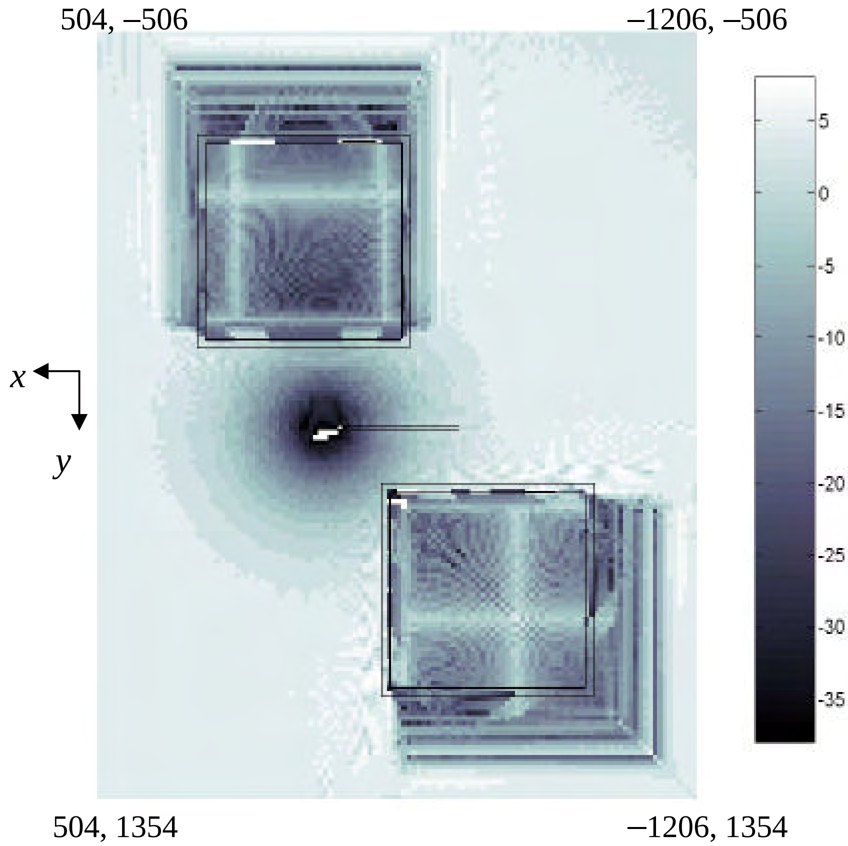


Figure 16. Two single level buildings with barrier wall with a UAV at (−50 inches, 450 inches, 400 inches).

## IV. SUMMARY AND CONCLUSIONS

UAV-GCS linkage in an urbanized area is subjected to multipath interference due to reflection, diffraction, and scattering. Shadow regions are formed when LOS areas are blocked. However, diffraction at corners causes illumination behind walls, below towers, and spreading through small apertures, that can actually help extend propagation in some cases.

This research focused on the signal contours generated when UAVs transmit towards an urbanized target area. Specific examples were shown to illustrate the effects of varying operating frequency, operating altitude, material composition of the building structures, and number of deployed UAVs on the signal contours. The examples are extracted from a larger set of data that can be found in references [9] and [11].

The signal strength level necessary for establishing a link will depend on the receiver sensitivity of the GCS. Once the GCS antenna and receiver characteristics are specified, the observation cells that satisfy the minimum signal strength requirements are easily identified by the color contours.

The simulation results indicate that in order to adapt to the dynamic propagation environment, an UAV deployed for MOUT must have the inherent capability to hover or fly at low speeds. Upon arriving at the pre-determined ideal location, the UAV will subsequently remain in situ for maximum coverage.

Operating at high frequency has merits of higher data rate transfer, which is crucial to support the large quantity of voice and live video feeds to be transmitted via UAV-GCS linkage. However, high frequencies are attenuated more rapidly in lossy materials like cement and glass commonly found in urbanized areas. At the same time, higher frequencies are more susceptible to attenuation due to weather such as rain, snow, and fog.

This research indicates that there exists an optimal operating altitude of UAV for signal coverage. Perching at rooftops to minimize power consumption may not be ideal, as most of the signals will simply be reflected upwards. If the UAV is positioned too high above buildings, the path loss becomes high and the areas beneath the UAV experience low signal levels when using a vertical monopole antenna (due to a downward pointing null in its radiation pattern).

Urbanized areas are made up of mostly straight roads lined with buildings. Through simulation, the locations of urban canyons can be identified and exploited. Meanwhile, identified shadow regions can either be avoided or illuminated by deploying ACNs. When limited to the use of a single UAV, it was found that operating a three times the height of the tallest building in the central city provides concentric, uniform coverage.

This research has established the process that can be used to predict the signal levels in an urban environment. By understanding the unique propagation modes possible in an urban environment, planners for MOUT will be able to provide continuous, uninterrupted and constant signal linkage between all the nodes (troops, artillery, planes, ships, sensors, etc). Using UAVs as ACNs will allow the edge in information dominance.

## V. REFERENCES


[1] United States Office of the Secretary of Defense, “Unmanned aerial vehicles roadmap 2002 – 2027,” pp. 33, December 2002.

[2] United States Office of the Secretary of Defence/C3I, “Unmanned aerial vehicles as communications platforms,” pp. 52, November 1997.

[3] J. B. Andersen, T. S. Rappaport, and S. Yoshida, “Propagation measurements and models for wireless communications channels,” *IEEE Commun. Mag*., Vol. 33, No. 1, pp. 42 – 29, January 1995.

[4] C. A. Balanis, *Antenna Theory, Analysis and Design*, second edition, Wiley, 1997.

[5] C. A. Balanis, *Advanced Engineering Electromagnetics*, Wiley, 1989.

[6] D. C. Jenn, *Radar and Laser Cross Section Engineering*, AIAA Education Series, 1985

[7] *Urbana Wireless Tooslset*, Training Manual, SAIC (DEMACO)

[8] http://www.spawar.navy.mil/robots/air/amgsss/mssmp.html accessed on 11 November 2003.

[9] Lock Wai Lek, “Effects of Radio-Wave Propagation in Urbanized Areas on UAV-GCS Command and Control,” Masters Thesis, Naval Postgraduate School, Monterey, CA, December 2003.

[10] J. Griffiths, *Radio Wave propagation and Antennas*, Prentice-Hall International (UK), 1987.

[11] F. Pala, “Frequency and Polarization Diversity Simulations for Urban UAV Communication and Data Links,” Masters Thesis, Naval Postgraduate School, Monterey, CA, September 2004.